A combination of transformation optics and surface impedance modulation to design compact retrodirective reflectors

Hassan Haddad, Renaud Loison, R. Gillard, A. Harmouch, A. Jrad

A combination of transformation optics and surface impedance modulation to design compact retrodirective reflectors

H. Haddad[1, 2, a)], R. Loison[1], R. Gillard[1], A. Harmouch[2], A. Jrad[3]
[1]*IETR, INSA-Rennes, 35708 Rennes, France*
[2] *CRSI, Faculty of engineering, Lebanese University, EDST,1300 Tripoli, Lebanon*
[3] *LEPA, Faculty of Sciences, Lebanese University, EDST,1301 Tripoli, Lebanon*

This study proposes a new approach to flatten retrodirective corner reflectors. The proposed method enables compact reflectors via Transformation Optics (TO) combined with Surface Impedance Modulation (SIM). This combination permits to relax the constraints on the anisotropic material resulting from the TO. Phase gradient approach is generalized to be used within anisotropic media and is implemented with SIM. Different reflector setups are designed, simulated and compared for $f_{op} = 8GHz$ using ANSYS® HFSS® in order to validate the use of such a combination.

I. INTRODUCTION

In recent years, increasing interest in compact reflectors with retrodirective response is observed[1]. Such devices can reflect electromagnetic waves in the anti-parallel direction of the incident wave. They are considered for applications like radar tracking and identification. Traditionally, a retrodirective reflector[2] is designed using a corner reflector structure that consists of two orthogonal metallic plates. Yet, this conventional reflector is too bulky to be integrated within most applications. Recent approaches have proposed Transformation Optics (TO) as a way to flatten the reflector[3,4]. However, most of these attempts lead to inhomogeneous anisotropic materials filling the inside volume of the reflector. These configurations while attractive and theoretically close in performance to the classical reflector, are either very complex or unattainable with current manufacturing technologies.

In our recent study[5], a more practical implementation of the TO compression compared to previous works, has been demonstrated. Indeed, the considered transformation leads to a homogeneous uniaxial anisotropic medium while keeping the same performance as the corner reflector. Even though a simplified medium is obtained, it is still difficult to manufacture, particularly because of the strong anisotropic factor it involves.

On the other hand, another flattening approach was proposed in [6, 7]. These studies are based on using two reflect-array-like panels assembled in a symmetrical dihedral form. In this topology, a convenient phase gradient is applied over the panels by printing small reflecting elements on their surface. More generally, it could be implemented by modulating the surface impedance of the reflecting panels (SIM). Indeed, it is well known that such a phase gradient introduces abnormal reflection over the surface[8] and that enables us to control the direction of the reflected wave. The obtained phase gradient is thus optimized to redirect the wave towards the source, after a double reflection on the panels. However, this mechanism appears to be quite sensitive to the incident angle[9] and the performance rapidly deteriorates as it increases.

This paper proposes a new flattening technique based on combining the TO approach presented in [5] and the phase gradient approach implemented with SIM.

The objective of the proposed combination is to mitigate the TO limitations by relaxing the constraints on the required anisotropic medium. In addition, it leads to improved results compared to the phase gradient approach alone. More generally, it provides a unified way to control the reflected wave from an object by acting on both its surface and volume.

II. THEORY

A. Derivation of the Phase Gradient

The starting scenario, that represents one panel of the reflector, is depicted in Fig.1. An x-polarized plane wave (TM) propagating along $+y$ impinges on the reflective panel lying along the Ox' axis. The inclination angle of the panel with respect to the horizontal axis is noted as α and is directly related to the flattening factor of the reflector ($\alpha = 45°$ for the unflattened corner reflector).

[a)] Corresponding author email: hassan.haddad@insa-rennes.fr

The whole domain is filled with a homogeneous anisotropic medium with the following relative constitutive parameters:

$$[\varepsilon_r] = \begin{bmatrix} \varepsilon_x & 0 & 0 \\ 0 & \varepsilon_y & 0 \\ 0 & 0 & \varepsilon_z \end{bmatrix} \text{ and } [\mu_r] = \begin{bmatrix} \mu_x & 0 & 0 \\ 0 & \mu_y & 0 \\ 0 & 0 & \mu_z \end{bmatrix} \quad (1)$$

In this medium, the respective wavenumbers and impedances are given by:

$$k_x = k_0\sqrt{\varepsilon_y\mu_z} \text{ and } \eta_x = \eta_0/\sqrt{\mu_z/\varepsilon_y} \quad (2)$$

for a wave polarized along y and propagating along x and

$$k_y = k_0\sqrt{\varepsilon_x\mu_z} \text{ and } \eta_y = \eta_0/\sqrt{\mu_z/\varepsilon_x} \quad (3)$$

for a wave polarized along x and propagating along y.

We now derive the required phase gradient over the panel in order to reflect the incident plane wave in the $+x$ direction.

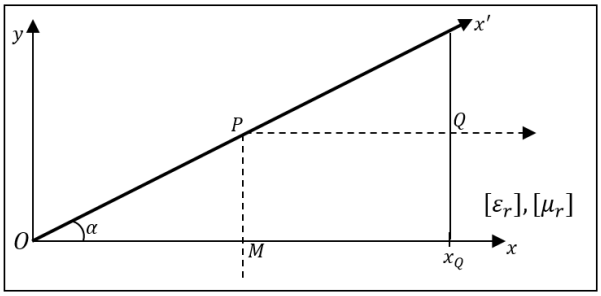

FIG. 1. General configuration with one inclined panel in an anisotropic medium.

Let's consider the phase of the incident wave at any point $M(x, 0)$ located on the Ox axis is zero. At point $P(x, x\tan\alpha)$ over the panel, the phase becomes:

$$\phi_P(x) = -k_y\, x \tan\alpha \quad (4)$$

Now assuming the reflection on the panel generates an additional phase $\phi_\Gamma(x')$ and enforcing propagation along $+x$ for the reflected wave, the phase at point Q (see Fig. 1) is:

$$\phi_Q(x) = -k_y\, x\, \tan\alpha - k_x(x_Q - x) + \phi_\Gamma(x') \quad (5)$$

where $x' = x/\cos\alpha$ and x_Q is an arbitrary x-coordinate for Q. In order to obtain a reflected wave propagating as a plane wave, this phase must not be dependent on x. Consequently, the additional phase over the panel is deduced as:

$$\phi_\Gamma(x') = k_y\, x' \sin\alpha - k_x\, x' \cos\alpha + \phi_0 \quad (6)$$

where $\phi_0$is an arbitrary phase constant.

It is interesting to note that (6) defines a linear phase variation: as in [9], it suggests a phase gradient is required on the reflecting surface to control the direction of the reflected wave. Using (2) and (3), it can be shown the phase gradient we obtain here is related to the properties of the filling medium and the inclination angle:

$$\frac{d\phi_\Gamma(x')}{dx'} = k_0\sqrt{\mu_z}\left(\sqrt{\varepsilon_x}\sin\alpha - \sqrt{\varepsilon_y}\cos\alpha\right) \quad (7)$$

Two different particular cases can be deduced from this generalized expression of the required phase gradient:

- If $\sqrt{\varepsilon_x/\varepsilon_y} = \cot\alpha$, it is found that:

$$\frac{d\phi_\Gamma(x')}{dx'} = 0 \quad (8)$$

In this case, no phase gradient is needed on the panel and a simple metallic plate is thus sufficient. Indeed, all the phase compensation at the point Q is provided by the sole anisotropic medium. This corresponds to the situation where flattening is obtained by TO only, as in [5].

- If $k_y = k_x = k_0$ (which means the considered medium is free space), (7) reduces to:

$$\frac{d\phi_\Gamma(x')}{dx'} = k_0(\sin\alpha - \cos\alpha) \qquad (9)$$

In this case, only the phase law over the panel is used to compensate for the phase differences at Q. This corresponds to the situation where flattening is obtained by SIM only, as in [9].

B. Trade-off between Anisotropic Factor and Phase Gradient

Previous particular cases correspond to extreme situations where only one approach (either TO or SIM) is used to flatten the corner reflector. Indeed, (7) demonstrates the possibility to combine both and suggests a trade-off can be achieved. This trade-off has to be made between the anisotropic factor a of the medium, defined as $a = \varepsilon_x/\varepsilon_y$, and the phase gradient $(\mathrm{d}\phi_\Gamma(x')/\mathrm{d}x')$ over the panels. In the following and as in [5], we consider the simple case where the anisotropic medium is homogeneous where b is considered constant with uniaxial constitutive parameters and we note:

$$[\varepsilon_r] = [\mu_r] = \begin{bmatrix} b & 0 & 0 \\ 0 & \frac{b}{a} & 0 \\ 0 & 0 & b \end{bmatrix} \qquad (10)$$

Fig. 2 displays the required phase gradient versus the anisotropic factor for $b = 2$ with different values of the inclination angle α.

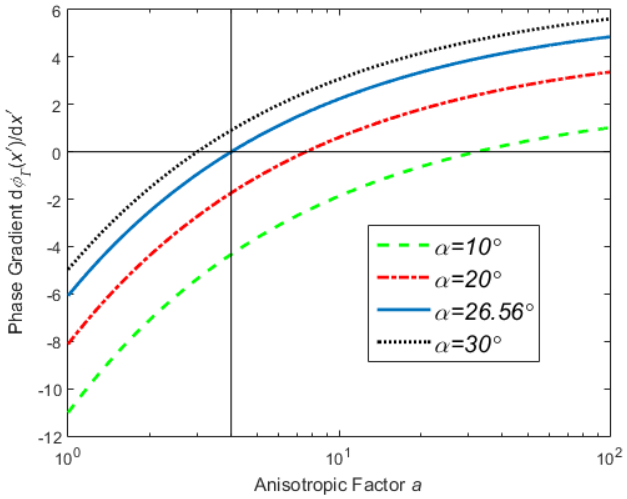

FIG. 2. Phase gradient versus the anisotropic factor for flattened reflector for different inclination angles α.

It clearly shows the anisotropic factor can be relaxed at the cost of a large phase gradient (in absolute value). On the other hand, no phase gradient is needed $(\mathrm{d}\phi_\Gamma(x')/\mathrm{d}x' = 0)$ if the anisotropic factor is set to the appropriate value. As an example, the case where α=26.56° and $a = 4$ (blue uniform line in Fig. 2) is the one that was studied in [5]. Note that smaller α corresponds to higher compressions of the corner reflector and logically lead to more stringent constraints on both the phase gradient and anisotropic factor. Finally, it must be higligthed that the case where the phase gradient is positive is useless: it corresponds to the situation where the compression brought by the anisotropic factor is too large and has to be compensated by an un-compression reaction on the panels.

III. NUMERICAL RESULTS

The flattened retrodirective reflector is now implemented using the approach developed in this letter. Numerical validations are carried with HFSS simulations.

A. Implementation of the Generalized Phase Gradient

The general configuration of the compact reflector is depicted in Fig. 3.

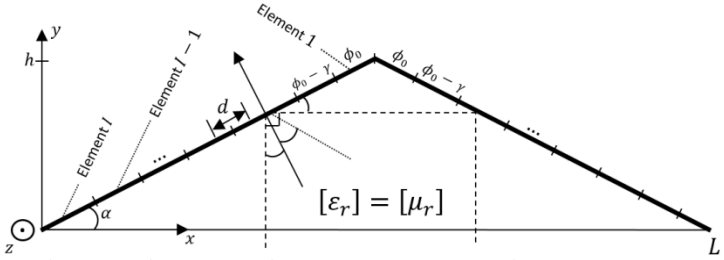

FIG. 3. General configuration of a compact reflector with a combination of Impedance modulation and a TO domain.

In the numerical implementation, the phase gradient is discretized, which means each panel is divided into I elements with length d and the applied phase shift on element i is:

$$\phi_{\Gamma_i} = \phi_{\Gamma_1} - (i-1)\gamma \qquad (11)$$

with γ the phase increment between consecutive elements:

$$\gamma = \frac{d\phi_\Gamma(x')}{dx'} d \qquad (12)$$

For the sake of simplicity and with no loss of generality, the phase shift on each element is set by tuning its surface impedance Z_{si} to the appropriate value. Assuming TM polarization, the reflection coefficient on element i is:

$$\Gamma_i = \frac{\frac{Z_{si}}{Z_{TM}} - 1}{\frac{Z_{si}}{Z_{TM}} + 1} \qquad (13)$$

where $Z_{\mathrm{TM}} = \eta_0 \cos\alpha$, η_0 being the free space wave impedance of the surrounding medium and α standing for the incident angle on the panel (equal to the inclination angle). Now, enforcing that $Z_{\mathrm{si}} = jX_{\mathrm{si}}$ is purely reactive so that all the power is reflected and noting that ϕ_{Γ_i} is the phase of Γ_i, it comes:

$$X_{si} = \frac{Z_{TM}}{tan\left(\frac{\phi_{\Gamma_i}}{2}\right)} \qquad (14)$$

Finally, by combining (14) and (11), the required surface impedance on each element for a given phase gradient is obtained.

B. Comparison of Different Configurations

For validation, we consider a reflector working at $f = 8\mathrm{GHz}$ with inclination angle $\alpha = 26.56°$ ($\cot\alpha = 2$), length $L = 20\lambda_0$, width $w = 10\lambda_0$ along the z axis and height $h = 5\lambda_0$, λ_0 being the wavelength in free space (see Fig. 3). Each panel is divided into $I = 44$ elements with $d = \lambda_0/4$. These parameters were carefully chosen so that the discretized phase gradient provides a precise enough approximation of (7) while maintaining reasonable computational resources for the simulations.
As detailed in Table I, different configurations are studied using different combinations of anisotropic factor a and phase increment γ.

TABLE I. Parameters used for simulated Configurations.

Reflector Configurations	Config. 1	Config. 2	Config. 3	Config. 4
Distribution constant b	1	2		
Anisotropic Factor a	1	2	3	4
Phase Increment γ	$-40.26°$	$-33.36°$	$-12.47°$	$0°$

Configuration 1 corresponds to the extreme situation where the flattening is only due to the modulation of the surface impedance on the panels (no anisotropic medium) while configuration 4 is the opposite with only TO (no phase gradient on the panels). Configurations 2 and 3 are intermediary cases combining both methodologies.
For simulations, the incident wave is applied on the left panel with a Gaussian beam of width $3\lambda_0$. The obtained near field maps are presented in Fig. 4. On these maps, the incident field in free space is not depicted.

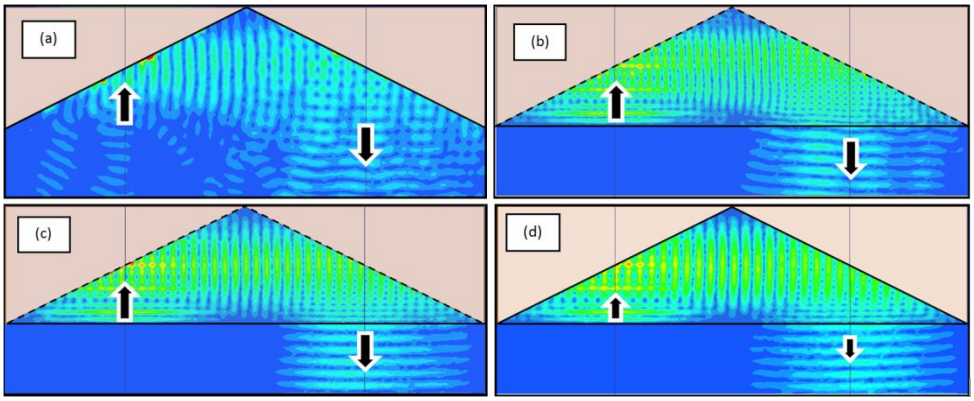

FIG. 4. Nearfield maps (time domain) for compact retro-directive reflector using (a) config. 1, (b) config. 2, (c) config. 3, (d) config. (4).

In particular, Fig. 4.(a) represents only the reflected field from the panels since this configuration is entirely in free space. On the other hand, Fig. 4.(b, c and d) show the incident Gaussian beam within the anisotropic medium superposed with the reflected fields from the left panel.
Globally, all configurations exhibit a retrodirective behavior with a reflected Gaussian beam coming from the right panel and propagating downwards. However, the retrodirective behavior is obviously better when the importance of TO with regards to SIM is increased. Next paragraph will provide more quantitative results.

C. RCS Response

A radar target (in our case the retrodirective reflector, see Fig. 5) is characterized by its radar cross section[10] (RCS) σ that gives the ratio of scattered power to incident power density. For a monostatic configuration (i.e. incident and reflected angles identical), σ is defined by:

$$\sigma(\theta) = \lim_{r\to\infty} 4\pi r^2 \left|\frac{E_r}{E_i}\right|^2 \qquad (15)$$

where $|E_i|$ and $|E_r|$ are the magnitude of the incident and reflected electric fields while r is the distance between the source and the target.

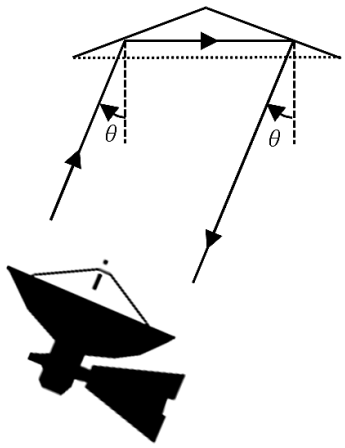

FIG. 5. Concept of RCS in one specific direction θ for the reflector configs presented in table 1.

Fig. 6 presents monostatic RCS for each of the reflector configurations. For comparison, the RCS of a classical corner reflector and of a metallic sheet (with the same effective area) are also given.

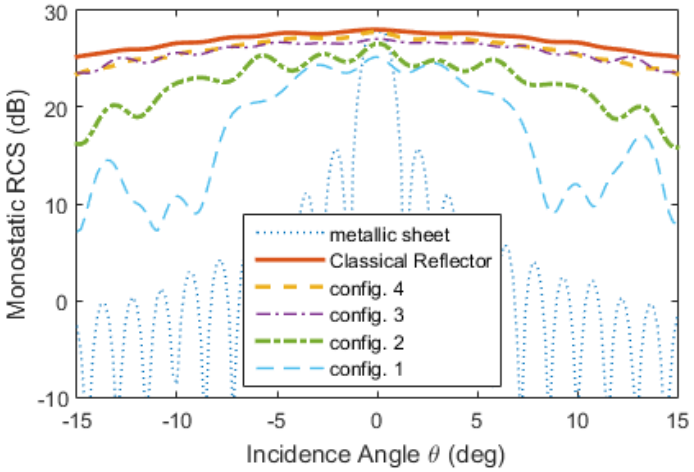

FIG. 6. RCS response for different reflectors versus incidence angle θ.

Table II gives the RCS levels at $\theta = 0°$ along with the half-power beam width (HPBW) for the configs used in Fig. 6.

TABLE II. Main performance for the different reflectors.

RCS Simulations	Metallic Sheet	Classical Reflector	Config. 1	Config. 2	Config. 3	Config. 4
RCS Level at $\theta = 0°$ (dB)	28.2	28.2	25.2	27.2	28.02	28.1
HPBW (degrees)	2.72°	38°	14°	28°	30°	34°

As can be seen, all flattened reflectors (config. 1 to 4) have a better beamwidth than the metallic sheet, which demonstrates the achieved retrodirective behavior is not limited to normal incidence. Although their maximum RCS level is a bit lower and none of them reaches the performance of the classical corner reflector, one should have in mind the overall thickness of the reflector has been reduced by a factor 2. Config. 4 is the best flattened structure, which shows the performance is improved (for both maximum level and beamwidth) when the anisotropic factor is increased. This is consistent with the fact that the flattening approach relying on SIM is quite sensitive to incident angle[9]. These results show that a small amount of SIM can significantly relax the anisotropic factor without affecting the performance too much, especially when skipping from configuration 4 to 3, with a 1.5 reduction factor in the anisotropy.
The RCS versus frequency at θ=0° is given in fig. 7 for config. 3.

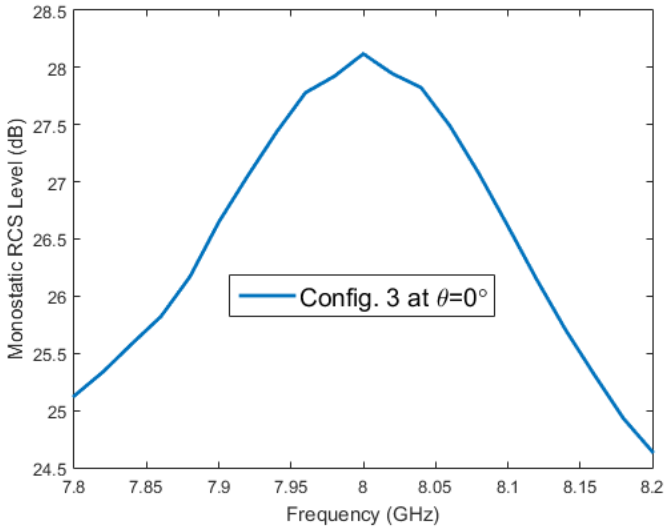

FIG. 7. RCS ($\theta = 0°$) response for config. 3 versus frequency.

The bandwith is quite narrow (2.25% for a 1dB decrease), which can be explained by the fact the phase gradient in the SIM approach has been optimized here for a single frequency (8GHz).

IV. CONCLUSION

A new approach to flatten retrodirective reflectors has been presented. It combines TO with SIM, providing a unified tool for controling the reflected wave from an object by acting on both its surface and its volume material properties.
A generalized phase gradient has been derived theoretically for the reflecting panels, accounting for the presence of an inner anisotropic media. The capability to perform a trade-off between anisotropic factor and phase gradient when designing a reflector has thus been demonstrated. This offers a new degree of freedom to improve performance while relaxing the constraints on required materials.
Simulations with HFSS have confirmed the expected retrodirective behavior is achieved for all tested configurations. They have also shown the introduction of a small dose of SIM is beneficial to reduce the anisotropic factor required by pure TO while maintaining the overall performance.

ACKNOWLEDGMENT

This work was supported by CEDRE program, AZM-UL program and IETR, INSA-Rennes.

REFERENCES

[1] D. S. Goshi K. M. K. H. Leong and T. Itoh, IEEE Radio and Wireless Symposium, pp.459-462 (2006).
[2] J. Kraus, R. Marhefka, 3rd ed. Mc Graw Hill. ISBN 0-07-112240-0, pp. 365 (2002).
[3] Shuai, Yijun, Tian, Junming, AIP Advances, 3 (2013).
[4] Y. Luo, L. He, S. Zhu, Helen L. W. Chan, Y. Wang, Phys. Rev. A 84, 023843 (2011).
[5] H. Haddad, R. Loison, R. Gillard, A. Jrad, A. Harmouch., MECAP2016, Beirut, Lebanon, IEEE, pp.1–4 (2016).
[6] D. Lipuma, S. Meric, R. Gillard, IET Electronic Letters, Vol. 49, Issue 2, pp.152 –154, (2013).
[7] I.L. Morrow, K. Morrison, M. Finnis, and W. Whittow., *LAPC*, Loughborough, IEEE, pp.1–4 (2015).
[8] N. Yu, P. Genevet, M.A. Kats, F. Aieta, J.-P. Tetienne, F. Capasso, Z. Gaburro, Science 334, pp.333–337 (2011).
[9] H. Srour, R. Gillard, S. Méric and D. Seetheramdoo, Ant. & Prop. Conference *LAPC*, Loughborough, IEEE, pp.1-4 (2016).
[10] E. F. Knott, J. Shaeffer, and M. Tuley, 2nd ed. SciTech Publishing (2004).